ACBD6 protein controls acyl chain availability and specificity of the *N*-myristoylation modification of proteins[S]

Eric Soupene[1] and Frans A. Kuypers

Children's Hospital Oakland Research Institute, Oakland, CA

Abstract **Members of the human acyl-CoA binding domain-containing (ACBD) family regulate processes as diverse as viral replication, stem-cell self-renewal, organelle organization, and protein acylation. These functions are defined by nonconserved motifs present downstream of the ACBD. The human ankyrin-repeat-containing ACBD6 protein supports the reaction catalyzed by the human and *Plasmodium* *N*-myristoyltransferase (NMT) enzymes. Likewise, the newly identified *Plasmodium* ACBD6 homologue regulates the activity of the NMT enzymes. The relatively low abundance of myristoyl-CoA in the cell limits myristoylation. Binding of myristoyl-CoA to NMT is competed by more abundant acyl-CoA species such as palmitoyl-CoA. ACBD6 also protects the *Plasmodium* NMT enzyme from lauryl-CoA and forces the utilization of the myristoyl-CoA substrate. The phosphorylation of two serine residues of the acyl-CoA binding domain of human ACBD6 improves ligand binding capacity, prevents competition by unbound acyl-CoAs, and further enhances the activity of NMT.[JLR] Thus, ACBD6 proteins promote *N*-myristoylation in mammalian cells and in one of their intracellular parasites under unfavorable substrate-limiting conditions.**—Soupene, E., and F. A. Kuypers. **ACBD6 protein controls acyl chain availability and specificity of the *N*-myristoylation modification of proteins. *J. Lipid Res.* 2019.** 60: **624–635.**

Supplementary key words protein acylation • membranes • phospholipids • binding protein • protein interaction

The *N*-myristoylation modification of specific proteins at an N-terminal glycine residue affects the activity of the myristoylated proteins, modulates their association with membranes, and mediates oligomeric assembly and the interaction with other proteins (1–4). *N*-Myristoylation occurs mainly during the translation of nascent peptides after the removal of the initiator methionine by methionyl aminopeptidase and the exposure of a glycine. The activity of *N*-myristoyltransferase (NMT) enzymes 1 and 2 is essential for human protein function. Likewise, *N*-myristoylation is of crucial importance for the intracellular development of pathogens such as parasitic protozoa, fungi, and viruses (5–12). *N*-Myristoylation is a multistep process initiated by the binding of myristoyl-CoA to the N-terminal domain of apo-NMT, covalent linkage of the myristoyl chain to the glycine residue, and release of CoA, followed by the final release of the acyl peptide. In retinal photoreceptor cells, $C_{14:1}$ and $C_{14:2}$ rather than $C_{14:0}$ are the fatty acids used to modify proteins such as the α-subunit of the G-protein photoreceptor (13–15). While the 14-carbon chain is the preferred substrate, NMT proteins lack binding specificity for C_{14}-CoA. This renders NMT incapable of preventing the unwarranted occupation of the site by acyl-CoA species other than C_{14}-CoA (4–6, 10, 13). Because the transfer rate of acyl chains with a length other than C_{14} is extremely slow, binding of the "wrong" acyl-CoA blocks the myristoyltransferase cycle for NMT enzymes. In the cell, the greater abundance of acyl-CoAs such as C_{16}-CoA compared with C_{14}-CoA would therefore prevent protein myristoylation. It follows that mechanisms that prevent binding or trigger the release of these nontransferable competitors from the myristoyl-CoA binding site are essential in supporting NMT enzyme activity.

Acyl-CoA binding domain-containing (ACBD) proteins are involved in the maintenance of diverse cellular functions. They interact with a multitude of proteins and can be located in the cytosol, organelles, or nucleus; bound to membranes; or secreted (16, 17). This protein family regulates processes as diverse as neural stem-cell self-renewal, protein and lipid acylation, lipid homeostasis, intracellular vesicle trafficking, organelle formation, viral replication, and apoptotic response (18–35). Plant ACBD proteins are also implicated in essential functions such as embryogenesis and resistance to various stresses (36–38). Acyl-CoAs

Manuscript received 28 November 2018 and in revised form 10 January 2019.

Published, JLR Papers in Press, January 14, 2019
DOI https://doi.org/10.1194/jlr.M091397

Abbreviations: ACB, acyl-CoA binding; ACBD, acyl-CoA binding domain-containing; ACN, acetonitrile; Glu, glutamate; hACBD6, human ACBD6; hNMT2, human NMT2; NMT, *N*-myristoyltransferase; PfNMT, *Plasmodium falciparum* *N*-myristoyltransferase; P-Ser, phosphoserine; αH, α helix.

[1]To whom correspondence should be addressed.
e-mail: esoupene@chori.org

[S] The online version of this article (available at http://www.jlr.org) contains a supplement.

bind to the N-terminal acyl-CoA binding (ACB) domain, and various motifs present at the carboxyl terminal of the different members of this family appear to define independent and nonredundant physiological functions of the ACBD proteins. The requirement and role of the acyl-CoA ligand bound to the ACB domain in the interaction with other proteins is poorly understood. The phosphorylation of two serine residues of α-helix 4 of the ACB domain of ACBD6 was detected in vivo, but the effect on its activity has not been determined (39, 40).

We previously showed that ACBD6 stimulated the activity of NMT2 and prevented the competition of the NMT reaction by C_{16}-CoA (26). An interaction between ACBD6 and NMT2 is required, and ligand binding to ACBD6 further enhanced its stimulatory effect on NMT2. Mutants of ACBD6 deficient in ligand binding did not stimulate the activity of NMT2. They also could not protect this enzyme from the competitor C_{16}-CoA. In the NMT2/ACBD6 complex, the acyl-CoA carrier appears to prevent the access of C_{16}-CoA and allows C_{14}-CoA to reach the acyl-transferase binding site in the presence of more abundant acyl-CoA. ACBD6 also interacts with NMT1 and likely regulates its activity.

The effect of the phosphorylation of Ser^{106} and Ser^{108} on the acyl-CoA binding property of ACBD6 and on the myristoyltransferase reaction was determined. We established that human ACBD6 (hACBD6) enhanced the activity of the malaria parasite *Plasmodium falciparum* NMT (PfNMT) enzyme. Although C_{12}-CoA was a stronger competitor of C_{14}-CoA than C_{16}-CoA for the parasite myristoyltransferase enzyme, hACBD6 also protected PfNMT from inhibition by the shorter acyl-CoA species. An ankyrin-repeat-containing acyl-CoA binding protein of *Plasmodium*, PfACBD6, was identified. Like the human homologue, PfACBD6 stimulates the activity of PfNMT. We propose that an essential role for ACBD6 proteins is to maintain substrate availability for the myristoyltransferase reaction and to provide specificity for C_{14}-CoA in the presence of competing acyl chains that are +2 or −2 carbon atoms different in length.

MATERIALS AND METHODS

Materials

O-Phospho-L-serine, acyl-CoAs, and fatty acids were from Sigma-Aldrich. All compounds used were reagent grade. The peptide GLYVSRLF (C-terminal amide; molecular mass of 953.16) was synthesized by YenZym Antibodies, LLC.

Cloning and site-directed mutagenesis

P. falciparum 3D7 NMT (1.2 kbp; gene ID: 811708) and ACBD6 (1.1 kbp; gene ID: 810744) cDNAs were cloned by RT-PCR. Total RNA was isolated from a frozen parasite sample (gift of Elizabeth S. Egan) with the PureLink RNA Mini Kit (Invitrogen). PfNMT was cloned in the pET28 vector (Novagen) with a hexahistidine tag at the N-terminal end. Using the same cloning strategy for PfACBD6 resulted in abundant unfinished translation products. A predicted transmembrane-spanning segment at the N-terminal end of the protein was removed, and a truncated construct (Met1 to Leu23) carrying a hexahistidine tag at the carboxyl end was successfully produced. Site-directed mutagenesis experiments were performed with the QuikChange Lightning Site-Directed Mutagenesis Kit (Agilent Technologies) according to the manufacturer's instructions. Primers were designed with the QuikChange Primer Design Program. The presence of the intended nucleotide change(s) and the absence of unwarranted mutations were verified by full-length sequencing of the constructs. ACBD6, N-terminally tagged with GFP, mutants, and truncated forms, were made in the pAcGFP1-C1 vector (Clontech Laboratories, Inc.). To produce the ACBD6 forms phosphorylated on Ser^{106} and Ser^{108}, the codons AGC^{106} and AGC^{108} were changed to the stop codon TAG. The constructs were cotransformed with pKW2.EF.Sep (41) into the *Escherichia coli* strain BL21(DE3)ΔserB (Addgene catalog no. 34929) (41, 42). For mammalian two-hybrid experiments, human NMT2 (hNMT2) and PfNMT were cloned into the pBIND vector, and hACBD6 was cloned into the pACT vector (Check-Mate Mammalian Two-Hybrid System; Promega), as previously described (26). HEK293 cells grown in 48-well plates were cotransfected with 200 ng of the constructs and the reporter pLuc at a pACT-pBIND-pLUC ratio of 2.25:0.25:0.5. Measurements were performed after 48 h of transfection with the Dual-Glo Luciferase Assay System (Promega).

Protein expression and purification

Human ACBD1, ACBD3, ACBD6, and NMT2 were produced as previously described (26–28, 43). Human ACBD4 and ACBD5 were cloned in pETM41 and produced as maltose binding protein fusion forms (gift of Joseph Costello) (19) in RosettaDE3 cells (Novagen). The production of ACBD6 forms phosphorylated on Ser^{106}, Ser^{108}, or on both of these serine residues was performed in *E. coli* grown in LB medium supplemented with 2 mM phosphoserine (41, 42). PfNMT and PfACBD6 were expressed in RosettaDE3. Although a large portion of PfNMT formed aggregates, the addition of 1% CHAPS during lysis of the cells and to the soluble fraction throughout the purification procedure was successful in maintaining PfNMT in solution. PfACBD6 was maintained in solution by the addition of 1% Triton X-100 in all buffers during the extraction and purification steps. Human ACBD1, ACBD3, ACBD6, NMT2, PfNMT, and PfACBD6 were purified by affinity metal chromatography. Human ACBD4 and ACBD5 were purified with amylose resin (New England BioLabs, Inc.). Purified ACBD1–6 proteins were stored at −80°C in 50 mM Tris-HCl (pH 8.0), 0.1 M NaCl, 5 mM EDTA, and 10% glycerol (v/v). Human NMT2 was stored in the same buffer in the presence of 0.2% Triton X-100. PfNMT was stored in 50 mM Tris-HCl (pH 8.0), 0.1 M NaCl, 5 mM EDTA, 1% CHAPS, and 20% glycerol to prevent the loss of activity. PfACBD6 was stored in 50 mM Tris-HCl (pH 8.0), 0.1 M NaCl, 5 mM EDTA, 10% glycerol, and 1% Triton X-100.

Binding, competition, and displacement assays

[^{14}C]$C_{18:1}$-CoA binding by ACBD proteins was performed as previously described (27). For competition experiments, unlabeled acyl-CoA was mixed with [^{14}C]$C_{18:1}$-CoA prior to the addition of the protein. Concentrations of ligands, competing acyl-CoA species, and proteins are indicated in the legend of each figure. The displacement of ACBD6-bound [^{14}C]$C_{18:1}$-CoA by unlabeled acyl-CoA was performed by purifying the [^{14}C]$C_{18:1}$-CoA/ACBD6 complex, removing unbound [^{14}C]$C_{18:1}$-CoA, and mixing the complex with competing acyl-CoA (see below). ABCD6 (1 μM) protein was incubated with 5 μM [^{14}C]$C_{18:1}$-CoA in 500 μl for 20 min at 37°C. The reaction was chilled on ice, and ACBD6 was pulled down with 50 μl NTA 50% slurry at 4°C for 10 min. The resin was washed 3 times in binding buffer and eluted with 50 μl 0.6 M imidazole. Ten microliters of the eluate were then added to 240 μl buffer containing 0–10 μM C_{24}-CoA. The displacement experiments were performed with 5 μM [^{14}C]$C_{18:1}$-CoA and 0.5, 1,

2, and 4 μM ACBD6 in 500 μl. The purified complex was then exposed to 2.5 μM C_{24}-CoA. Following incubation for 20 min at 37°C, ACBD6 was then pulled down a second time with 60 μl NTA 50% slurry and washed as above. The amount of [^{14}C]$C_{18:1}$-CoA left in the ACBD6 bound-resin fraction was quantified with a scintillation counter.

N-Myristoyltransferase activity measurements

Real-time measurements of released CoA from acyl-CoAs by purified NMT forms were performed at 30°C in a Cary Varian Cary 50 UV-Vis spectrophotometer in the presence of 200 μM Ellman's reagent as previously described (26). Detection and quantification of the formation of the acyl peptide in the presence of acyl-CoAs and the peptide GLYVSRLF was performed by separation on a Luna 5u C18 100A HPLC column (250 × 4.6 mm; Phenomenex) and monitoring of the absorbance of the tyrosine residues at 274 nm. Reactions were performed in 20 mM sodium phosphate (pH 8.0), 1 mM EDTA, 1% CHAPS, and 200 μM peptide with concentrations of C_{14}-CoA from 5 to 50 μM. The volume of the reactions, the concentrations of C_{14}-CoA and competing acyl-CoA, the NMT enzyme, and the ACBD proteins are indicated in the legend of each figure. Reactions were performed at 37°C and were stopped at various times by adding 1.08 vol ice-cold methanol/TFA 8%. Samples were vortexed and precipitated on ice for 20 min. Proteins were removed by centrifugation at 8,000 *g* for 10 min at 4°C. The supernatants containing the peptide and acyl peptide were collected and dried down under vacuum overnight at 20°C. The pellets were suspended in 50% methanol/TFA 4% (v/v; from 30 to 80 μl). A 10 μl sample was injected onto the C18 column, and separations were performed as described previously (10, 44, 45). An acetonitrile (ACN) gradient was generated in the presence of 0.1% TFA and HPLC-grade water. Samples were loaded onto the column equilibrated with 10% ACN/TFA 0.1%. The ACN concentration was increased to 68% in 30 min at a flow rate of 1 ml per minute and to 100% in 1 min at 1.5 ml/min. After 3 min at 100% ACN/TFA 0.1%, the ACN concentration was decreased to 10%, and the column was equilibrated for 10 min at 1 ml/min. The percentage of product formed, detected by absorbance of the peptide at 274 nm, is reported as the relative volume of the myristoyl peptide peak (34.5 min) relative to the sum of the volume of the peptide peak (18 min) and of the acyl peptide detected in each injected sample. In one experiment, the reaction was performed in the absence of added C_{14}-CoA but in the presence of the bound C_{14}-CoA/ABCD6 complex. ACBD6 (20 μM) was incubated with 100 μM C_{14}-CoA for 20 min at 37°C. The bound complex was pulled down as described above, and the 50 μl eluate was incubated with 60 μg PfNMT and 200 μM peptide for 2 h at 37°C in 1 ml buffer. A control reaction was performed with the eluate obtained from the pull down of C_{14}-CoA incubated in the absence of ACBD6. Calculations and statistical analysis were performed with GraphPad Prism 7.

Cell culture and transfection

HeLa229 cells, obtained from ATCC (CCL-2.1), were maintained in MEM α (Invitrogen) containing 10% FBS and 2 mM glutamine. For microscopy studies, cells were grown and transfected with Turbofect (Thermo Fisher Scientific) on 12 mm round coverslips (Electron Microscopy Sciences) in 24-well plates (46). Imaging was performed with a Keyence microscope equipped with a 40× objective.

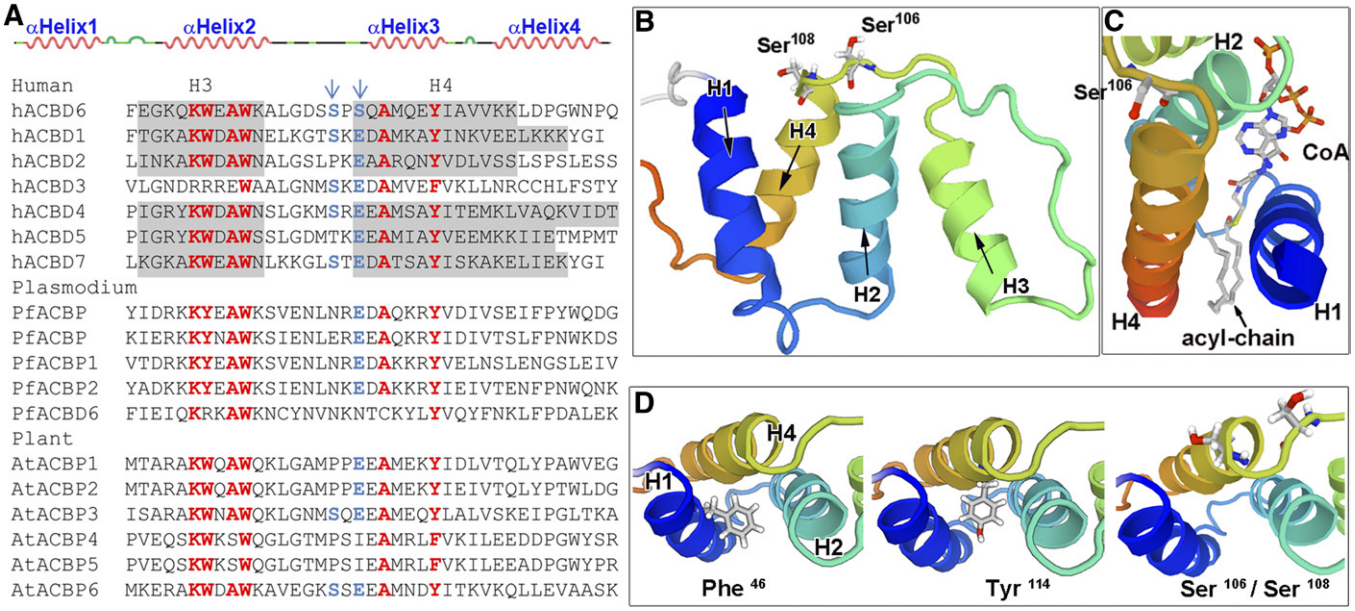

Fig. 1. Phosphorylated ACBD6 serine residues are not conserved in ACBD members. A: The amino acid alignment of the α-helixes 3 and 4 (H3, H4) of the ACB domain of the ACBD members of the human, *P. falciparum*, and *Arabidopsis thaliana* family is shown. Some of the highly conserved residues are shown in red. A cartoon representation of the four α-helices of the ACB domain of hACBD6 is presented above the alignment. The phosphorylated residues Ser^{106} and Ser^{108}, shown in blue, are indicated with a blue arrow. Substitution of Ser^{108} to a Glu residue in some forms is also shown in blue. The position of α-helixes 3 and 4 of hACBD members is highlighted in gray and was obtained from the deposited structures in the Protein Data Bank (www.rcsb.org) for ACBD1 (DBI; PDB:2FJ9), ACBD2 (ECI2; PDB:4U18), ACBD4 (PDB:2WH5), ACBD5 (PDB:3FLV), ACBD6 (PDB:2COP), and ACBD7 (PDB:3EPY). B: NMR structure resolution of the ACB domain of hACBD6 (PDB:2COP). Note that Ser^{108} is positioned at the top of the pocket formed by α-helixes 1, 2, and 4. C: Structure of the ACB domain of hACBD4 complexed with stearoyl-CoA (PDB:2WH5) is presented to indicate the role of the groove formed by α-helixes 1 and 4 in binding the acyl chain. D: The two aromatic residues Phe46 (α-helix l) and Tyrl 14 (α-helix 4), whose substitution to alanine significantly reduced the binding capacity of hACBD6 (27) and the two phosphorylated residues Ser^{106} and Ser^{108} are shown. Note that the two aromatic residues protrude in the inside of the pocket involved in binding of the acyl chain.

Ser^{106} and Ser^{108} of hACBD6 are not essential for ligand binding

Two serine residues located in the acyl-CoA binding domain of hACBD6, Ser^{106} and Ser^{108}, are phosphorylated in vivo (26, 39, 40). Ser^{106}, near the fourth α helix (αH4; S108 to K120), is present in some ACBD forms of humans and plants but not in the *Plasmodium* proteins, including the homologue PfACBD6 (**Fig. 1A**, B). Ser^{108}, at the beginning of αH4, is not conserved, but most ACBD proteins carry a glutamate (Glu) residue at this position. Glu can structurally mimic the presence of a phosphoserine, which might indicate that the activity of unphosphorylated ACBD6 could be different from phospho-ACBD6. The acyl chain of the acyl-CoA ligand is bound in the cavity formed by αH1, αH2, and αH4, and the CoA head group faces αH2 in the proximity of αH3 (Fig. 1C). Site-directed mutagenesis of conserved residues in the four α helices of ACBD6 identified two aromatic residues, Phe46 of αH1 and Tyr114 of αH4, whose substitution to alanine had the most influence in acyl-CoA binding (27). Based on the structure, these two residues protrude in the acyl-chain binding cavity, and Ser^{106} and Ser^{108} are located at the top of the pocket.

The substitution of the two serine residues to alanine generated ACBD6 forms with similar binding affinity compared with the native ACBD6 (**Fig. 2A**). However, a significant decrease in binding capacity was detected, which indicates that although neither Ser^{106} nor Ser^{108} are essential, they are implicated in binding. The substitution and truncation of the serine residues did not appear to affect the cellular location of GFP-tagged forms (Fig. 2B). Deleting an entire α helix, αH4, also had no apparent effect. Thus, the phosphorylation of Ser^{106} and Ser^{108}, as well as ligand binding, do not appear to be essential for the cytosolic and nuclear localization of hACBD6 in the cell.

Serine phosphorylation enhances ligand binding capacity of hACBD6

Phospho-Ser^{106} (P-Ser^{106}), P-Ser^{108}, and P-Ser^{106}/P-Ser^{108} ACBD6 forms were produced in *E. coli* and purified (see Materials and Methods). The binding activity of the phosphorylated forms was determined by competition experiments in the presence of radiolabeled [^{14}C]C$_{18:1}$-CoA (i.e., ligand) and unlabeled acyl-CoAs (i.e., competitors). Competition depends on the binding affinity of the protein for its ligand and competitor. As expected, the decreased binding of the radiolabeled acyl-CoA was a function of the relative concentration of ligand to competitor at a given protein concentration (**Fig. 3**). At ligand concentrations close to the observed K_d of ~10 μM (Fig. 2A), the binding of the ligand was sensitive to the presence of the competitor, and the addition of acyl-CoA of various chain lengths resulted in lower binding values (Fig. 3A). Competition was observed with assays performed with the unphosphorylated form hACBD6 and the double-mutant Ser$^{106/}$Ser^{108}-Ala. However, with the double-phosphorylated P-Ser^{106}/P-Ser^{108} form, binding of the ligand [^{14}C]C$_{18:1}$-CoA was higher in the presence of the competitor (Fig. 3A). This phenomenon was observed for all five acyl-CoAs tested, even when unlabeled C$_{18:1}$-CoA was added to [^{14}C]C$_{18:1}$-CoA. In addition, each of the single phosphorylated forms, P-Ser^{106} and P-Ser^{108}, also showed increased ligand binding in the presence of competitors (Fig.3B). To render ligand binding competition of P-Ser^{106}/P-Ser^{108} dependent on the total concentration of acyl-CoAs present in the reaction, titration experiments were performed in the presence of a fixed concentration of the competitor, resulting in the strongest effect on binding, C$_{24}$-CoA (Fig.3A), and with increasing concentrations of the ligand [^{14}C]C$_{18:1}$-CoA. Limited amounts of protein were also used, and under such conditions no binding could be detected at the lowest ligand concentrations in the absence of the competitor (Fig. 3C,

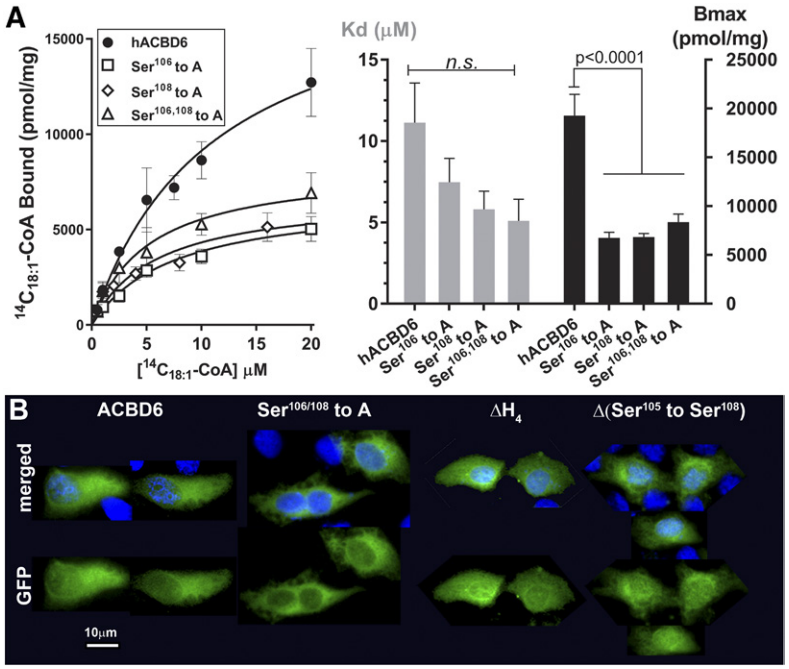

Fig. 2. Phosphorylated ACBD6 serine residues are not essential. Ser^{106} and Ser^{108} of hACBD6 were changed to alanine residues to generate the single Ser^{106}-A, Ser^{108}-A, and double Ser$^{106/108}$-A constructs. A: Binding activity was measured with 2 μM protein and increasing concentrations of [^{14}C]C$_{18:1}$-CoA (0–20 μM). Error bars represent the standard deviations of four measurements. The binding parameters K_d and B_{max} are summarized in the graph bar on the right. B: The GFP-tagged constructs of hACBD6, the double-mutant Ser$^{106/108}$-A, a truncated form of α-helix4 (ΔH4), and a form truncated from Ser^{105} to Ser^{108} (ΔSer^{105} to Ser^{108}) were transfected in HeLa cells. Cells were fixed after 24 h, and the nuclei were stained with the Hoechst dye (blue). Images of the GFP (lower) and merged signal of GFP with Hoechst staining (upper) are shown. Note that images of various GFP-positive cells detected on the slides were manipulated and combined to generate the panel.

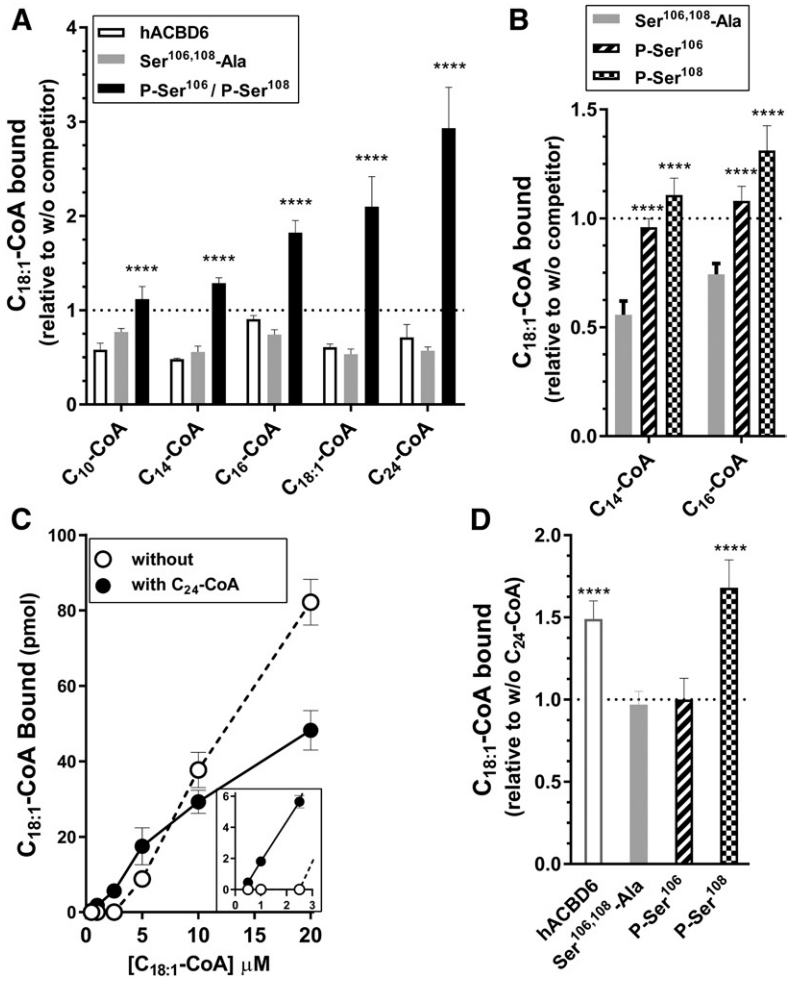

Fig. 3. Phosphorylated ACBD6 serine residues enhanced binding capacity. A: Binding assays were performed with 1 μM hACBD6, $Ser^{106/108}$-A, and the phosphorylated protein $P\text{-}Ser^{106}$/$P\text{-}Ser^{108}$ in the presence of 5 μM [^{14}C]$C_{18:1}$-CoA and 5 μM of the indicated acyl-CoA species. Control reactions were performed in the absence of the competitors, and values obtained in their presence are presented relative to the values obtained in their absence. B: Assays were performed as in panel A with the single phosphorylated proteins $P\text{-}Ser^{106}$ and $P\text{-}Ser^{108}$ and the mutant form $Ser^{106/108}$-A. C: Binding titration assays were performed with 0.3 μM $P\text{-}Ser^{106}$/$P\text{-}Ser^{108}$ protein and increasing concentrations of [^{14}C]$C_{18:1}$-CoA (0.5–20 μM) in the absence (opened circles) or presence (filled circles) of 5 μM C_{24}-CoA. Values obtained with ligand concentrations ⩽2.5 μM are plotted at a different scale in the inset. D: Binding assays were performed with 0.3 μM of the indicated proteins and with 2.5 μM [^{14}C]$C_{18:1}$-CoA in the absence or presence of 5 μM C_{24}-CoA. Values obtained in the presence of the competitor are presented relative to those obtained in its absence. Error bars in the four plots represent the standard deviations of six measurements. ****$P = 0.0001$.

inset). However, the addition of the competitor increased binding of the ligand from the lowest concentration (0.5 μM) to concentrations closest to the K_d (Fig. 3C). Competition did occur when the concentration of ligands reached a K_d of 10 μM. To a lesser degree, this behavior was also observed with the unphosphorylated form under the limiting ligand concentration of 2.5 μM (Fig. 3D).

Acyltransferase activity of NMT enzymes is stimulated by hACBD6

The interaction of NMT2 with hACBD6 enhances the myristoyl-CoA esterase (26) and myristoyltransferase activity of the enzyme (**Fig. 4**). hACBD6 stimulation of myristoyl peptide formation occurs even under very limiting conditions (Fig. 4B) and in the presence of the competitor palmitoyl-CoA (C_{16}-CoA) (Fig.4C). hACBD6 increases both the rate and yield of production of the acyl peptide and protects binding of the substrate myristoyl-CoA (C_{14}-CoA) to NMT from competition. To determine whether the role of hACBD6 was limited to the human myristoyltransferase enzyme, the activity of PfNMT was determined (**Fig. 5**). As observed for NMT2, hACBD6 stimulates PfNMT activity, and the increased formation of the myristoyl peptide in its presence was greater under substrate-limiting conditions (up to 40-fold) (Fig. 5C, D). The interaction was significantly weaker than with NMT2, but an hACBD6/PfNMT complex appears to have formed in the cells (supplemental Fig. S1A). An hACBD6 form with truncated ankyrin-repeat motifs (ACBD6ΔC-ter) did not associate with either PfNMT or NMT2. A mutant form affected in ligand binding and carrying the 4 substitution in the ACB domain (FFKY-to-A) (27) also fails to interact with PfNMT. This mutant protein interacted with hNMT2, suggesting that complex formation with the *Plasmodium* enzyme might require the acyl-CoA-bound form of hACBD6.

ACBD6 compensates for lack of NMT specificity for the C_{14} acyl chain

The abundant C_{16}-CoA is a competitor of the myristoyltransferase reaction. hNMT2 cannot prevent binding of an acyl chain two carbon atoms longer than C_{14}-CoA, but the palmitoyl chain is not a substrate of the acyl-transferase reaction, and the enzyme cannot release it (4–6, 10). hACBD6 protects hNMT2 from C_{16}-CoA (Fig. 4C) (26). Although myristoyl peptide formation by PfNMT was also reduced in the presence of C_{16}-CoA, the -2 carbon species lauroyl-CoA (C_{12}-CoA) was far more inhibitory (**Fig. 6A**). Under a low C_{14}-CoA concentration (10 μM), a 2-fold C_{12}-CoA excess reduced the production of the myristoyl peptide by half, whereas a 12-fold excess of C_{16}-CoA was required (Fig. 6B, C). Measurements of the esterase activity of the enzyme confirmed that the two competitors bind and were processed

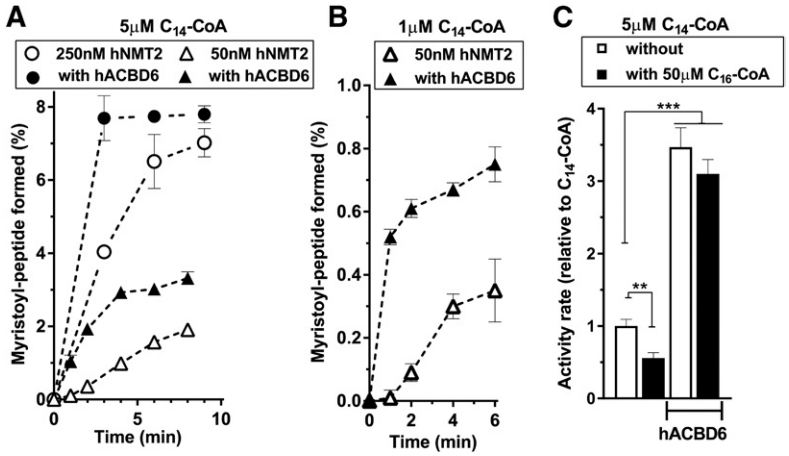

Fig. 4. Activity of NMT2 in the presence of hACBD6. Measurements of the formation of the myristoyl peptide were performed in the absence (open symbols) or presence (closed symbols) of 6 μM hACBD6 from 0 to 10 min at 37°C. Reactions were performed in 600 μl, and at the indicated time points 100 μl were removed and transferred into a solution of 50% methanol/TCA 0.1%. The peptide and myristoyl peptide were extracted and quantified by HPLC on a C18 column (see Materials and Methods). hNMT2 was added at a concentration of 250 nM (circle) and 50 nM (triangle) in the presence of 5 μM C_{14}-CoA (A) and at 50 nM in the presence of 1 μM C_{14}-CoA (B). The competitor C_{16}-CoA (50 μM) was added to the reaction mixtures containing 5 μM C_{14}-CoA and 50 nM NMT2 in the absence or presence of 6 μM hACBD6, as indicated (C). Activity rate values are presented relative to the value obtained in the absence of hACBD6 and C_{16}-CoA. Error bars in all three plots represent the standard deviations of values obtained from three reactions. $^{**}P < 0.005$ and $^{***}P < 0.001$.

by PfNMT (supplemental Fig. S1B). The presence of hACBD6 in the reaction protected the enzyme from the u sage of an acyl chain other than C_{14}. hACBD6 successfully relieved the inhibition by C_{16}-CoA and further increased product formation (Fig. 6B). C_{14}-CoA processing in the presence of C_{12}-CoA was also increased by hACBD6 (Fig. 6C).

A new acyl peptide peak was detected in the presence of C_{12}-CoA, and its formation increased as the levels of the C_{14} peptide peak dropped (Fig. 6A, **Fig. 7A**). The formation of the lauroyl peptide was differently affected by hACBD6 depending on the presence of the correct substrate C_{14}-CoA. In the absence of C_{14}-CoA, hACBD6 could not prevent PfNMT from processing C_{12}-CoA, and the reaction was nearly independent of its presence (Fig. 7B). In the presence of C_{14}-CoA, a 2-fold concentration excess of C_{12}-CoA resulted in a 2-fold reduction of myristoyl peptide, but in

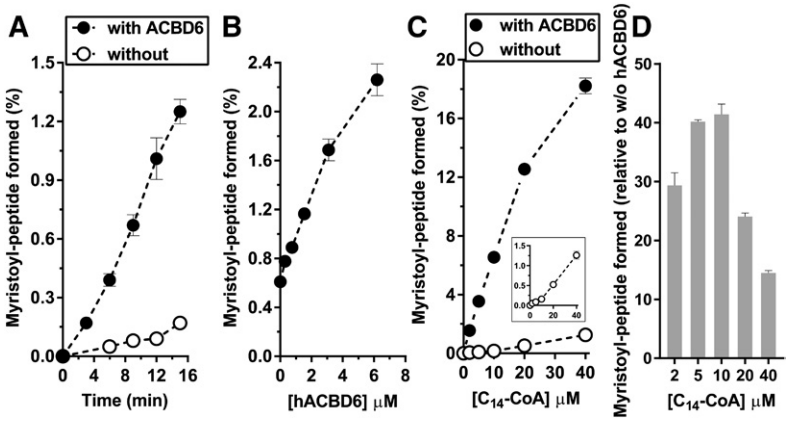

Fig. 5. hACBD6 supports PfNMT activity under substrate-limiting concentrations. A: Measurements of the formation of the myristoyl peptide were performed in the absence (open symbols) or presence (closed symbols) of 6 μM hACBD6 from 0 to 16 min at 37°C. PfNMT was added at a concentration of 250 nM in the presence of 10 μM C_{14}-CoA in 500 μl. At the indicated time points, 80 μl were removed and analyzed. B: Measurements were performed with 300 nM PfNMT in the presence of 10 μM C_{14}-CoA and increasing concentrations of hACBD6 (0–6 μM). Reactions were performed in 120 μl at 37°C for 2 h. C: Measurements were performed with 250 nM PfNMT in the absence or presence of 6 μM hACBD6 with increasing concentrations of C_{14}-CoA (0–40 μM). Reactions were performed in 120 μl at 37°C for 2 h. The plot of the low values obtained in the absence of hACBD6 is presented at a different scale in the inset. D: Values obtained in the presence of hACBD6 at the different C_{14}-CoA concentrations shown in panel C are presented relative to the values obtained in its absence. Note the higher fold change in activity at a low C_{14}-CoA concentration (≤10μM) compared with the saturating concentration (40 μM). Error bars in the four plots represent the standard deviations of values obtained from three reactions.

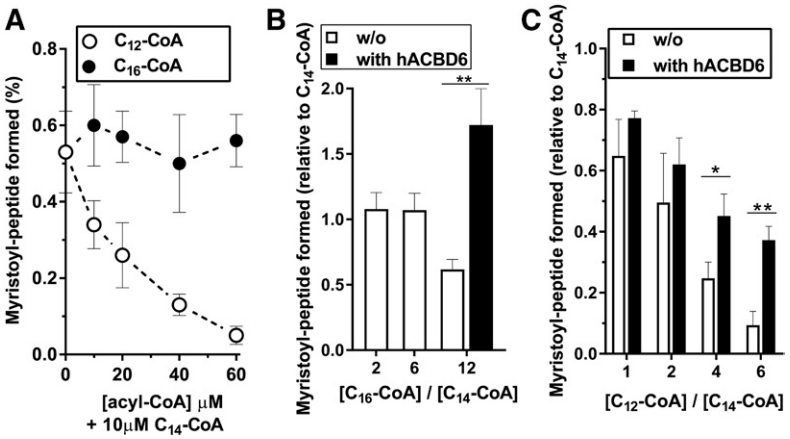

Fig. 6. hACBD6 protects PfNMT from acyl-CoA competition. Measurements of the formation of the myristoyl peptide were performed in the presence of 10 μM C_{14}-CoA and increasing concentrations of C_{16}-CoA (closed symbols) and C_{12}-CoA (open symbols) (A). Reactions were performed in 120 μl at 37°C for 20 min with 400 nM PfNMT. Activity values obtained with C_{16}-CoA and C_{14}-CoA or with C_{12}-CoA and C_{14}-CoA in the absence or presence of 10 μM hACBD6 are shown in panel B and panel C, respectively. Values obtained in the presence of the competitors are presented relative to values obtained from the reaction performed in their absence. Note that PfNMT is more sensitive to competition by C_{12}-CoA than by C_{16}-CoA. Error bars in the three plots represent the standard deviations of values obtained from three reactions. *$P < 0.05$ and **$P < 0.005$.

the presence of hACBD6, a 4-fold excess of C_{12}-CoA was required to achieve a 50% reduction (Fig.7C). In the presence of hABCD6, the increased preference of PfNMT for the C_{14} chain over the C_{12} chain was also confirmed by the decrease in C_{12} processing when the enzyme had the choice of acyl chains (Fig. 7C). Although when challenged with nonphysiological conditions (high concentration of C_{12}-CoA in the absence of C_{14}-CoA), hACBD6 had little to no detectable effect, it could slow the usage of the C_{12} chain by the PfNMT enzyme in a mixture containing C_{14}-CoA. These data established that ACBD6 can provide substrate specificity for the myristoyltransferase reaction and prevent the enzyme from processing the "wrong" but more abundant acyl-chain species under conditions that are likely encountered in vivo.

Plasmodium ankyrin-containing ACBD6 protein stimulates PfNMT activity

A search of PlasmoDB, a genome database for *Plasmodium* (plasmodb.org), retrieved five genes encoding putative acyl-CoA binding proteins (**Fig. 8A**). Three genes produced the shortest of the forms, homologous to the human ACBD1 (DBI) protein. The other two genes carry different motifs at the extended carboxyl-terminal end. PfACBP1 carries two conserved motifs implicated in export through the parasite membrane and localization in the erythrocyte: *Plasmodium* helical interspersed subtelomeric and *Plasmodium* ring-infected erythrocyte antigen N-terminal (47). On the basis of the presence of two ankyrin-repeat motifs downstream of the ACB domain, the unnamed product of the fifth gene was referred to as PfACBD6. A transmembrane-spanning segment motif was predicted at the N-terminal end and had to be removed for successful expression in *E. coli* (see Materials and Methods). A 60-residue-long motif, rich in lysine (12) and asparagine (26), is inserted between the second and third α-helix of the ACB domain (Fig. 8A). These poly-KN tracks are often found in *Plasmodium* proteins and reflect the AT-rich genome of the parasite (48, 49).

PfACBD6 is a functional protein and binds acyl-CoA (Fig. 8B, C). In addition, it stimulates the NMT activity of PfNMT and counters inhibition by C_{16}-CoA (Fig. 8D, supplemental Fig. 1B). Thus, the ankyrin-repeat containing acyl-CoA binding proteins of humans and *Plasmodium* regulate the NMT reaction.

Myristoyl-CoA bound to hACBD6 is a substrate of NMT

The ability of different members of the human acyl-CoA binding protein family to stimulate the myristoyltransferase reaction was determined. Of the five ACBD forms tested, hACBD6 was the most efficient in enhancing the production of the myristoyl peptide by PfNMT (**Fig. 9A**, B). ACBD1, ACBD3, ACBD4, and ACBD5 were able to stimulate PfNMT but to levels similar or lower than that of the ACBD6 mutant altered in acyl-CoA binding (FFKY-A form). The preference for the ACBD protein that interacts with the enzyme confirmed that complex formation improves

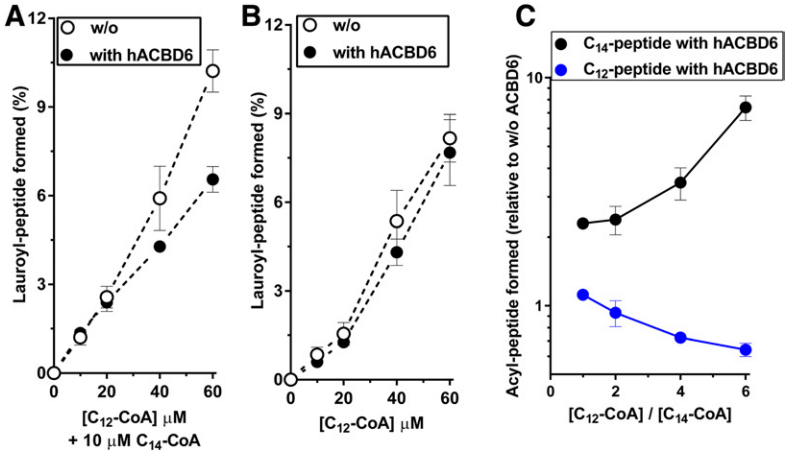

Fig. 7. hACBD6 enhances the specificity of PfNMT toward C_{14}-CoA. Measurements of the formation of the lauroyl peptide were performed with increasing concentrations of C_{12}-CoA in the presence (A) or absence (B) of 10 μM C_{14}-CoA. hACBD6 was added at a concentration of 10 μM. Values obtained at the different C_{12}-CoA concentrations in the presence of C_{14}-CoA and hACBD6 are presented relative to the values obtained in the absence of hACBD6 (C). Note the logarithmic scale of the plot in panel C. Error bars in the three plots represent the standard deviations of values obtained from three reactions.

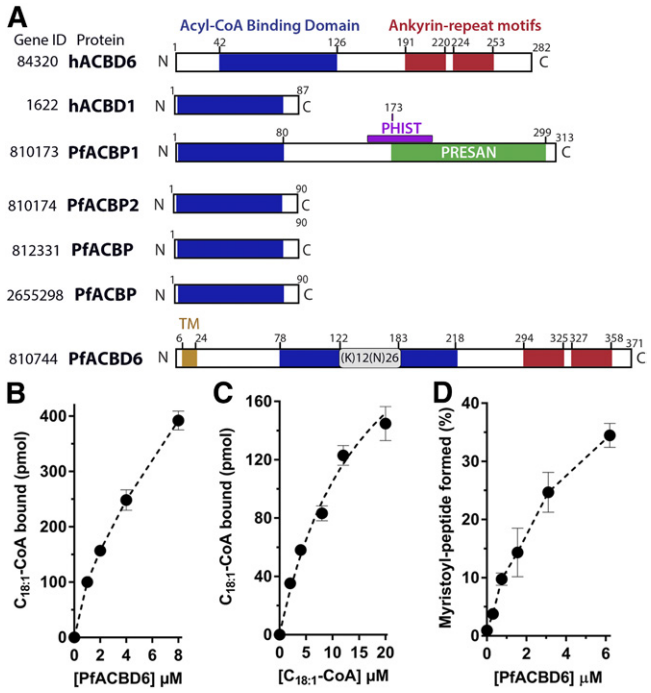

Fig. 8. Identification and activity of *Plasmodium* ACBD6 protein. A: Representation of the five predicted acyl-CoA binding proteins of *P. falciparum* 3D7. The shortest human form ACBD1 (DBI) and the human ankyrin-repeat containing ACBD6 protein are included as reference. The gene ID of each form is shown on the left. A predicted unnamed protein was identified as the *Plasmodium* homologue of hACBD6 and is referred to as PfACBD6. A transmembrane-spanning segment (TM) is predicted at its N-terminal end (yellow box). The acyl-CoA binding domain (blue) is extended due to the insertion of a region rich in Lys and Asp residues between the second and third α-helix of the domain (gray highlighted). Like the human form, PfACBD6 carries two ankyrin-repeat motifs (ANK) at the carboxyl-terminal end (red). PfACBP1 carries two motifs: *Plasmodium* helical interspersed subtelomeric (PHIST; purple) and *Plasmodium* ring-infected erythrocyte antigen N-terminal (PRESAN; green). B, C: Binding activity was determined with increasing concentrations of PfACBD6 (0–8 µM) in the presence of 20 µM [^{14}C] C18:1-CoA (B) and with increasing concentrations of [^{14}C]C18:1-CoA (0–20 µM) in the presence of 2 µM PfACBD6 (C). Error bars represent the standard deviations of four measurements. D: Measurements of the formation of the myristoyl peptide were performed with 300 nM PfNMT in the presence of 10 µM C_{14}-CoA and increasing concentrations of PfACBD6 (0–6 µM). Reactions were done in 80 µl at 37°C for 2 h. Error bars represent the standard deviations of values obtained from three reactions.

the ability of ACBD6 to enhance the myristoyltransferase reaction. The role of the binding activity of hACBD6 in the mechanism leading to increased NMT activity was investigated. The substrate C_{14}-CoA was incubated with hACBD6, and the C_{14}-CoA-bound hACBD6 complex was isolated from the unbound C_{14}-CoA left in the reaction. The purified C_{14}-CoA/ACBD6 was then fed to PfNMT in a buffer mixture lacking C_{14}-CoA. The formation of the myristoyl peptide under such reaction conditions established that the C_{14}-CoA bound to hACBD6 was available to the NMT (Fig. 9C). The isolation procedure was also performed with C_{14}-CoA in the absence of hACBD6, and no product was formed following the incubation with the enzyme (Fig. 9C).

The ability to deliver and transfer the C_{14}-CoA substrate from the acyl-CoA carrier to NMT allows the myristoyltransferase reaction to proceed efficiently, even at concentrations below the binding affinity of the enzyme. This would account for the greater stimulatory effect of hABCD6 observed under substrate-limiting concentrations compared with saturating conditions (Fig. 5D).

Phosphorylation-dependent stimulation of myristoylation

To further investigate the ability of hACBD6 to increase the availability of the substrate to the NMT enzyme, displacement experiments of ACBD6-bound ligand by acyl-CoA competitors were performed. The complex hACBD6/[^{14}C]$C_{18:1}$-CoA was isolated, and the amount of [^{14}C]$C_{18:1}$-CoA still bound to the protein following incubation with increasing concentrations of the competitor C_{24}-CoA was quantified (**Fig. 10A**). Compared with the hACBD6 form, phosphorylation of Ser^{106} and Ser^{108} residues protected the bound ligand, and a higher concentration of competitor was required to achieve 50% displacement. This observation was confirmed when increasing amounts of the ACBD6-ligand complex were exposed to a fixed concentration of competitor (Fig. 10B). Although the removal of the two serine residues did not influence the dissociation of the ligand, their phosphorylation resulted in significant resistance of ligand bound to the P-Ser^{106}/P-Ser^{108} ACBD6 form (Fig. 10C). The phosphorylated forms also further increased the activity of the PfNMT enzyme compared with ACBD6 (**Fig. 11**). Substitution of the two serines to glutamate residues (Ser^{106}/Ser^{108}-Glu) did not appear to produce a form that was as active as the phosphorylated serine forms.

Thus, the improved binding capacity of the phosphorylated hACBD6 form enhanced its ability to hold the bound ligand in a mixture of competing acyl-CoAs under similar conditions encountered in vivo. This property of hACBD6 gives C_{14}-CoA a competitive advantage in the presence of more abundant acyl-CoAs and provides the NMT enzyme with the correct substrate in the unfavorable cellular environment.

DISCUSSION

The NMT enzymes lack selectivity for myristoyl-CoA and display a binding affinity (~600 nM) that is significantly higher than the cellular concentration of this acyl-CoA, ranging from 5 to 200 nM. These findings imply that mechanisms exist to support the NMT reactions in the cell (2, 3, 50, 51). The use of a relatively low abundant acyl chain under those unfavorable cellular conditions strongly suggests that the covalent linkage of a myristate to an N-terminal glycine residue confers properties to the acylated proteins that the more abundant palmitate chain cannot provide. In fact, some proteins are palmitoylated and myristoylated, on N-terminal cysteine and glycine, respectively, which indicate that these two acyl modifications are not equivalent (52). In vitro, acyl-CoA species that are either two carbon atoms longer or shorter (C_{12}–C_{16}) bind with similar affinity than C_{14} (0.6–1.4 µM) and thus can compete for binding to

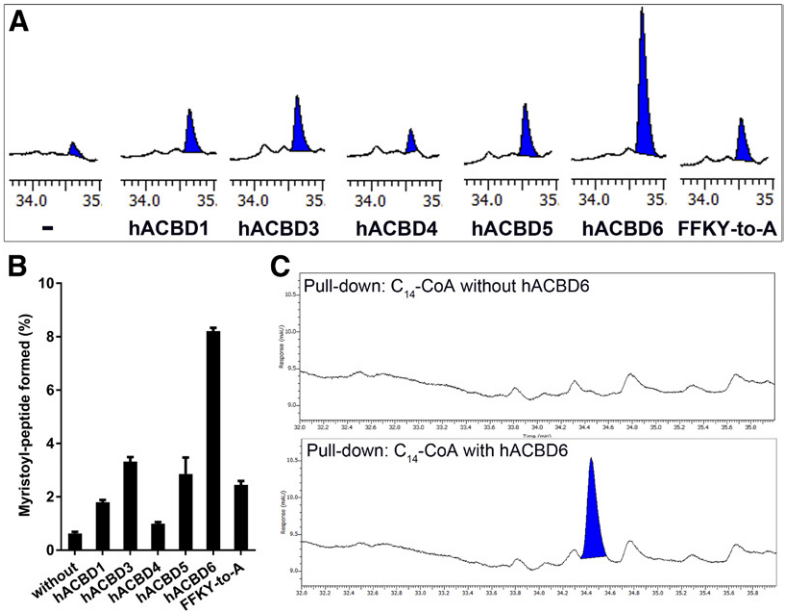

Fig. 9. C_{14}-CoA bound to hACBD6 is a substrate for the PfNMT enzyme. A: Measurements of the formation of the myristoyl peptide were performed in the absence or presence of 20 μM human ACBD1, ACBD3, ACBD4, ACBD5, and ACBD6 and the ACBD6 mutant FKKY-to-A. FKKY-to-A carries a substitution of the residues Phe[46], Lys[73], Lys[95], and Tyr[114] to alanine and displayed low binding capacity (27). The chromatogram traces obtained at 274 nm at the time of the elution of the C_{14}-peptide (blue peak; ∼34.5 min) from the C18 column are shown. Reactions were performed in 120 μl at 37°C for 2 h with 700 nM PfNMT in the presence of 10 μM C_{14}-CoA. B: The amount of the myristoyl peptide obtained in the experiments shown in panel A was quantified. Error bars represent the standard deviations of at least three reactions. C: hACBD6 (20 μM) was incubated with 100 μM C_{14}-CoA for 20 min at 37°C and then purified to remove the unbound C_{14}-CoA. The hACBD6/C_{14}-CoA complex was incubated with 1.25 μM PfNMT and 200 μM peptide in a 1 ml reaction for 2 h at 37°C (bottom chromatogram). A control reaction was performed with the pull-down sample obtained from C_{14}-CoA incubated in the absence of hACBD6 (top). The chromatogram traces obtained at 274 nm are shown, and the C_{14}-peptide is shown as a blue peak.

NMT (10). The transfer of acyl chains from the enzyme to the protein other than C_{14} is either blocked or very slow, which favors the addition of a myristate. However, occupation of the binding site by these acyl-CoA species would lead to the progressive inactivation of the enzyme because they could not be released once bound. The acyl-chain species bound to the enzyme also affect the interaction of NMT with the target proteins. The binding of acyl chains other than C_{14} can significantly increase the K_m binding affinity of NMT for the protein substrate (10). It has been established that, in vivo, the enzyme can preferentially transfer species other than $C_{14:0}$. In the retina, the unsaturated $C_{14:1}$ chain is the major species detected in myristoylated proteins. In addition, the polyunsaturated $C_{14:2}$

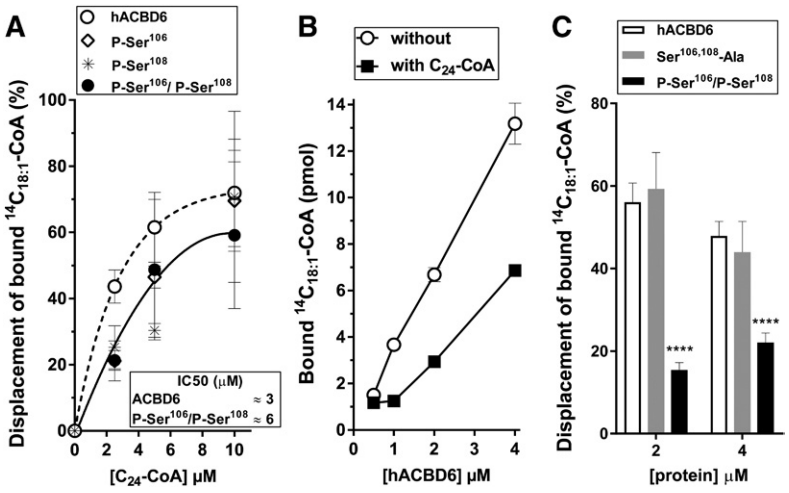

Fig. 10. Phosphorylation of hACBD6 prevents ligand displacement by competitor. Displacement of [^{14}C]$C_{18:1}$-CoA bound to the proteins was performed as described in the Materials and Methods section. A: hACBD6, P-Ser[106], P-Ser[106], and P-Ser[106]/P-Ser[108] proteins (1 μM) were incubated with 5 μM [^{14}C]$C_{18:1}$-CoA, and the ligand-protein complexes were isolated and incubated in the presence of increasing concentrations of C_{24}-CoA (0–10 μM). Amounts of [^{14}C]$C_{18:1}$-CoA still bound to the proteins in the presence of the competitor are presented in percentages relative to values obtained in its absence. The calculated concentration of C_{24}-CoA required to achieve 50% displacement of prebound [^{14}C]$C_{18:1}$-CoA to hACBD6 and P-Ser[106]/P-Ser[108] is shown in the inset. B: Displacement assays were performed at a fixed concentration of C_{24}-CoA (2.5 μM) with complexes isolated from the incubation of 5 μM [^{14}C]$C_{18:1}$-CoA with increasing concentrations of hACBD6 (0.5–4 μM). C: Displacement values obtained with 2 and 4 μM hACBD6, mutant Ser[106/108]-A, and phosphorylated P-Ser[106]/P-Ser[108] are presented in percentages relative to values obtained in the absence of C_{24}-CoA. Error bars in the three plots represent the standard deviations of values obtained from four reactions. ****$P = 0.0001$.

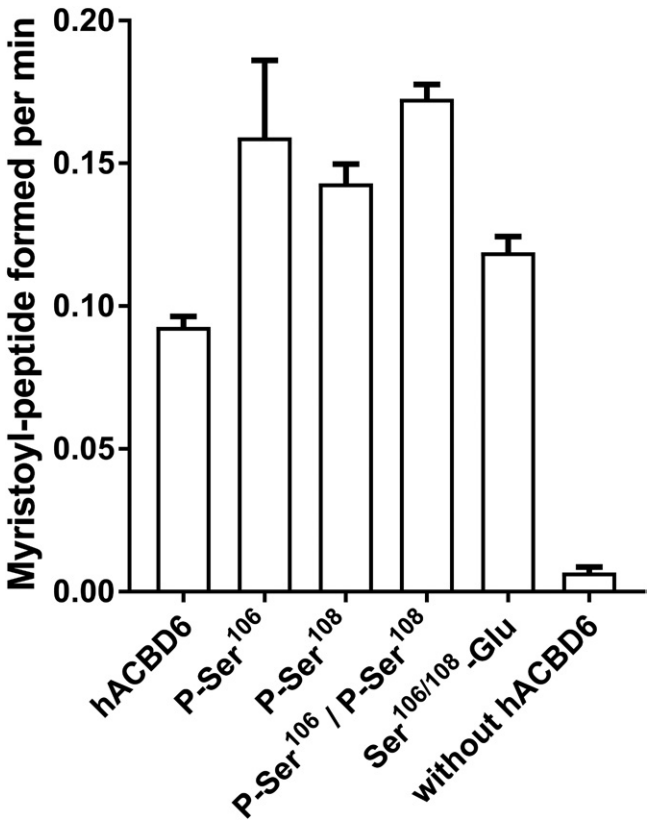

Fig. 11. Phosphorylation enhances the stimulation of NMT activity by hACBD6. Measurements of the formation of the myristoyl peptide were performed in the absence or presence of 6 μM hACBD6, P-Ser^{106}, P-Ser^{108}, P-Ser^{106}/P-Ser^{108}, and Ser$^{106/108}$-Glu, which carries the substitution of the residues Ser^{106} and Ser^{108} to Glu residues. Reactions were performed with 200 nM PfNMT in the presence of 10 μM C_{14}-CoA in 120 μl at 37°C for 3, 6, 9, 12, and 15 min. The rates of formation were calculated and are presented as the amounts of myristoyl peptide formed per minute. Error bars represent the standard deviations of three measurements.

and the shorter-chain C_{12}, expected to have a much slower transfer rate than $C_{14:0}$, are also detected in retinal proteins at similar levels compared to C_{14} (14). Thus, it appears that the NMT enzyme itself does not strictly control the acyl species used for *N*-myristoylation but that acyl-CoA availability in a given cell greatly affects the reaction (6). The finding that the acyl-CoA binding protein ACBD6 stimulated NMT activity and enhanced the specificity of the enzyme toward the myristate chain in the presence of other species suggests that ACBD6 is part of the cellular mechanism that regulates the *N*-myristoylation reaction.

Of the five ACBD proteins tested, ACBD6 was the most efficient in stimulating NMT activity, but other members of the ACBD family also were able to enhance the production of the myristoyl peptide in vitro. This provides evidence that systems affecting acyl-CoA availability affect NMT activity. ACBD6 appears to be the only member to also interact directly with NMT, and this unique property could account for its greater effect on myristoylation compared with the other ACBD members. The fact that both the human and *Plasmodium* ACBD6 proteins stimulated PfNMT also suggests that motifs that are located downstream from the conserved ACB domain are unique to the ankyrin-repeat motif-containing member of the ACBD family. Phosphorylation of the two serine residues of the ACB domain of ACBD6 has a significant positive effect on binding capacity and myristoyl peptide formation. Other ACBD proteins are phosphorylated in vivo, but although ACBD3 and ACBD5 have six and nine phosphorylated residues, respectively, none are located in the ACB domain (39, 40). The only two ACBD6 residues known to be phosphorylated are near and part of the fourth α-helix of the ACB domain. These serine residues are not conserved in the ACBD family, and Ser^{108} appears to be substituted by the phosphomimic Glu residue in other members. The effect of the phosphorylation of these serine residues on the properties of ACBD6 suggests that the activity of this member of the family is regulated in vivo. Cell-cycle global profiling of human phosphoproteins detected a specific upregulation of Ser^{106} and Ser^{108} phosphorylation during the M phase (39, 40). This finding strongly suggests that the function of the phosphorylated form of ACBD6 is increased during mitosis. Given the significant difference in NMT activity in the presence of phospho-ACBD6 compared with the unphosphorylated form, an increased need for protein myristoylation during that phase of the cell cycle could be possible.

Myristoylation of proteins occurs during translation after the removal of the initiator methionine on the nascent polypeptide. However, during apoptotic events, NMT enzymes can also modify proteolytically cleaved proteins after the exposure of an N-terminal glycine and a cryptic myristoylation motif (50, 51, 53). ACBD6 phosphorylation could also be increased during apoptosis to support the additional need for NMT activity. A variety of pathogens rely on protein acylation processes. The development of *P. falciparum* in erythroid cells is blocked by several chemicals that inhibit the action of the PfNMT enzyme (11, 12, 54, 55). The host and parasite ACBD6 regulate PfNMT activity, and the disruption of this process may provide an opportunity to block the parasite growth. In conclusion, our results provide evidence that ACBD6 proteins have an important role in the myristoylation of proteins in eukaryotic cells and support the substrate availability and selectivity of the NMT enzymes.

The authors thank Yonka Christova, Joseph Costello, and Elizabeth S. Egan for providing the vector pKW2 EF-Sep, MBP-ACBD4 and MBP-ACBD5 constructs, and a frozen sample of *P. falciparum*, respectively.

REFERENCES

1. Patwardhan, P., and M. D. Resh. 2010. Myristoylation and membrane binding regulate c-Src stability and kinase activity. *Mol. Cell. Biol.* **30:** 4094–4107.
2. Resh, M. D. 2013. Covalent lipid modifications of proteins. *Curr. Biol.* **23:** R431–R435.
3. Resh, M. D. 2016. Fatty acylation of proteins: the long and the short of it. *Prog. Lipid Res.* **63:** 120–131.
4. Wright, M. H., W. P. Heal, D. J. Mann, and E. W. Tate. 2010. Protein myristoylation in health and disease. *J. Chem. Biol.* **3:** 19–35.

5. Bhatnagar, R. S., K. Futterer, G. Waksman, and J. I. Gordon. 1999. The structure of myristoyl-CoA:protein N-myristoyltransferase. *Biochim. Biophys. Acta.* **1441:** 162–172.
6. Bhatnagar, R. S., O. F. Schall, E. Jackson-Machelski, J. A. Sikorski, B. Devadas, G. W. Gokel, and J. I. Gordon. 1997. Titration calorimetric analysis of AcylCoA recognition by myristoylCoA:protein N-myristoyltransferase. *Biochemistry.* **36:** 6700–6708.
7. Brannigan, J. A., B. A. Smith, Z. Yu, A. M. Brzozowski, M. R. Hodgkinson, A. Maroof, H. P. Price, F. Meier, R. J. Leatherbarrow, E. W. Tate, et al. 2010. N-myristoyltransferase from Leishmania donovani: structural and functional characterisation of a potential drug target for visceral leishmaniasis. *J. Mol. Biol.* **396:** 985–999.
8. Desmeules, P., S. E. Penney, B. Desbat, and C. Salesse. 2007. Determination of the contribution of the myristoyl group and hydrophobic amino acids of recoverin on its dynamics of binding to lipid monolayers. *Biophys. J.* **93:** 2069–2082.
9. Goncalves, V., J. A. Brannigan, D. Whalley, K. H. Ansell, B. Saxty, A. A. Holder, A. J. Wilkinson, E. W. Tate, and R. J. Leatherbarrow. 2012. Discovery of Plasmodium vivax N-myristoyltransferase inhibitors: screening, synthesis, and structural characterization of their binding mode. *J. Med. Chem.* **55:** 3578–3582.
10. Heuckeroth, R. O., L. Glaser, and J. I. Gordon. 1988. Heteroatom-substituted fatty acid analogs as substrates for N-myristoyltransferase: an approach for studying both the enzymology and function of protein acylation. *Proc. Natl. Acad. Sci. USA.* **85:** 8795–8799.
11. Tate, E. W., A. S. Bell, M. D. Rackham, and M. H. Wright. 2014. N-Myristoyltransferase as a potential drug target in malaria and leishmaniasis. *Parasitology.* **141:** 37–49.
12. Wright, M. H., B. Clough, M. D. Rackham, K. Rangachari, J. A. Brannigan, M. Grainger, D. K. Moss, A. R. Bottrill, W. P. Heal, M. Broncel, et al. 2014. Validation of N-myristoyltransferase as an antimalarial drug target using an integrated chemical biology approach. *Nat. Chem.* **6:** 112–121.
13. DeMar, J. C., Jr., and R. E. Anderson. 1997. Identification and quantitation of the fatty acids composing the CoA ester pool of bovine retina, heart, and liver. *J. Biol. Chem.* **272:** 31362–31368.
14. Dizhoor, A. M., L. H. Ericsson, R. S. Johnson, S. Kumar, E. Olshevskaya, S. Zozulya, T. A. Neubert, L. Stryer, J. B. Hurley, and K. A. Walsh. 1992. The NH2 terminus of retinal recoverin is acylated by a small family of fatty acids. *J. Biol. Chem.* **267:** 16033–16036.
15. Kokame, K., Y. Fukada, T. Yoshizawa, T. Takao, and Y. Shimonishi. 1992. Lipid modification at the N terminus of photoreceptor G-protein alpha-subunit. *Nature.* **359:** 749–752.
16. Fan, J., J. Liu, M. Culty, and V. Papadopoulos. 2010. Acyl-coenzyme A binding domain containing 3 (ACBD3; PAP7; GCP60): an emerging signaling molecule. *Prog. Lipid Res.* **49:** 218–234.
17. Neess, D., S. Bek, H. Engelsby, S. F. Gallego, and N. J. Faergeman. 2015. Long-chain acyl-CoA esters in metabolism and signaling: role of acyl-CoA binding proteins. *Prog. Lipid Res.* **59:** 1–25.
18. Chen, Y., S. Bang, S. Park, H. Shi, and S. F. Kim. 2015. Acyl-CoA-binding domain containing 3 modulates NAD+ metabolism through activating poly(ADP-ribose) polymerase 1. *Biochem. J.* **469:** 189–198.
19. Costello, J. L., I. G. Castro, C. Hacker, T. A. Schrader, J. Metz, D. Zeuschner, A. S. Azadi, L. F. Godinho, V. Costina, P. Findeisen, et al. 2017. ACBD5 and VAPB mediate membrane associations between peroxisomes and the ER. *J. Cell Biol.* **216:** 331–342.
20. Costello, J. L., I. G. Castro, T. A. Schrader, M. Islinger, and M. Schrader. 2017. Peroxisomal ACBD4 interacts with VAPB and promotes ER-peroxisome associations. *Cell Cycle.* **16:** 1039–1045.
21. Herzog, K., M. L. Pras-Raves, S. Ferdinandusse, M. A. T. Vervaart, A. C. M. Luyf, A. H. C. van Kampen, R. J. A. Wanders, H. R. Waterham, and F. M. Vaz. 2018. Functional characterisation of peroxisomal beta-oxidation disorders in fibroblasts using lipidomics. *J. Inherit. Metab. Dis.* **41:** 479–487.
22. Hua, R., D. Cheng, E. Coyaud, S. Freeman, E. Di Pietro, Y. Wang, A. Vissa, C. M. Yip, G. D. Fairn, N. Braverman, et al. 2017. VAPs and ACBD5 tether peroxisomes to the ER for peroxisome maintenance and lipid homeostasis. *J. Cell Biol.* **216:** 367–377.
23. Ishikawa-Sasaki, K., S. Nagashima, K. Taniguchi, and J. Sasaki. 2018. Model of OSBP-mediated cholesterol supply to Aichi virus RNA replication sites involving protein-protein interactions among viral proteins, ACBD3, OSBP, VAP-A/B, and SAC1. *J. Virol.* **92:** e01952-17.
24. Klima, M., D. Chalupska, B. Rozycki, J. Humpolickova, L. Rezabkova, J. Silhan, A. Baumlova, A. Dubankova, and E. Boura. 2017. Kobuviral non-structural 3A proteins act as molecular harnesses to hijack the host ACBD3 protein. *Structure.* 25**:** 219–230.
25. McPhail, J. A., E. H. Ottosen, M. L. Jenkins, and J. E. Burke. 2017. The molecular basis of Aichi virus 3A protein activation of phosphatidylinositol 4 kinase IIIbeta, PI4KB, through ACBD3. *Structure.* **25:** 121–131.
26. Soupene, E., J. Kao, D. H. Cheng, D. Wang, A. L. Greninger, G. M. Knudsen, J. L. DeRisi, and F. A. Kuypers. 2016. Association of NMT2 with the acyl-CoA carrier ACBD6 protects the N-myristoyltransferase reaction from palmitoyl-CoA. *J. Lipid Res.* **57:** 288–298.
27. Soupene, E., and F. A. Kuypers. 2015. Ligand binding to the ACBD6 protein regulates the acyl-CoA transferase reactions in membranes. *J. Lipid Res.* **56:** 1961–1971.
28. Soupene, E., D. Wang, and F. A. Kuypers. 2015. Remodeling of host phosphatidylcholine by Chlamydia acyltransferase is regulated by acyl-CoA binding protein ACBD6 associated with lipid droplets. *MicrobiologyOpen.* **4:** 235–251.
29. Yu, X. J., M. Liu, and D. W. Holden. 2016. Salmonella effectors SseF and SseG interact with mammalian protein ACBD3 (GCP60) to anchor salmonella-containing vacuoles at the Golgi network. *MBio.* **7:** e00474-16.
30. Elle, I. C., K. T. Simonsen, L. C. Olsen, P. K. Birck, S. Ehmsen, S. Tuck, T. T. Le, and N. J. Faergeman. 2011. Tissue- and paralogue-specific functions of acyl-CoA-binding proteins in lipid metabolism in Caenorhabditis elegans. *Biochem. J.* **437:** 231–241.
31. Onwukwe, G. U., P. Kursula, M. K. Koski, W. Schmitz, and R. K. Wierenga. 2015. Human Delta(3),Delta(2)-enoyl-CoA isomerase, type 2: a structural enzymology study on the catalytic role of its ACBP domain and helix-10. *FEBS J.* **282:** 746–768.
32. Ferreira, N. S., H. Engelsby, D. Neess, S. L. Kelly, G. Volpert, A. H. Merrill, A. H. Futerman, and N. J. Faergeman. 2017. Regulation of very-long acyl chain ceramide synthesis by acyl-CoA-binding protein. *J. Biol. Chem.* **292:** 7588–7597.
33. Fu, Y., X. Cui, S. Fan, J. Liu, X. Zhang, Y. Wu, and Q. Liu. 2018. Comprehensive characterization of toxoplasma acyl coenzyme A-binding protein TgACBP2 and its critical role in parasite cardiolipin metabolism. *MBio.* **9:** e01597-18.
34. Ryuda, M., S. Tsuzuki, H. Matsumoto, Y. Oda, T. Tanimura, and Y. Hayakawa. 2011. Identification of a novel gene, anorexia, regulating feeding activity via insulin signaling in Drosophila melanogaster. *J. Biol. Chem.* **286:** 38417–38426.
35. Majerowicz, D., H. K. Hannibal-Bach, R. S. C. Castro, B. L. Bozaquel-Morais, M. Alves-Bezerra, L. A. M. Grillo, C. A. Masuda, N. J. Faergeman, J. Knudsen, and K. C. Gondim. 2016. The ACBP gene family in Rhodnius prolixus: expression, characterization and function of RpACBP-1. *Insect Biochem. Mol. Biol.* **72:** 41–52.
36. Lung, S. C., and M. L. Chye. 2016. The binding versatility of plant acyl-CoA-binding proteins and their significance in lipid metabolism. *Biochim. Biophys. Acta.* **1861:** 1409–1421.
37. Xiao, S., and M. L. Chye. 2009. An Arabidopsis family of six acyl-CoA-binding proteins has three cytosolic members. *Plant Physiol. Biochem.* 47**:** 479–484.
38. Ye, Z. W., and M. L. Chye. 2016. Plant cytosolic Acyl-CoA-binding proteins. *Lipids.* **51:** 1–13.
39. Dephoure, N., C. Zhou, J. Villen, S. A. Beausoleil, C. E. Bakalarski, S. J. Elledge, and S. P. Gygi. 2008. A quantitative atlas of mitotic phosphorylation. *Proc. Natl. Acad. Sci. USA.* **105:** 10762–10767.
40. Olsen, J. V., M. Vermeulen, A. Santamaria, C. Kumar, M. L. Miller, L. J. Jensen, F. Gnad, J. Cox, T. S. Jensen, E. A. Nigg, et al. 2010. Quantitative phosphoproteomics reveals widespread full phosphorylation site occupancy during mitosis. *Sci. Signal.* **3:** ra3.
41. Rogerson, D. T., A. Sachdeva, K. Wang, T. Haq, A. Kazlauskaite, S. M. Hancock, N. Huguenin-Dezot, M. M. Muqit, A. M. Fry, R. Bayliss, et al. 2015. Efficient genetic encoding of phosphoserine and its nonhydrolyzable analog. *Nat. Chem. Biol.* **11:** 496–503.
42. Park, H. S., M. J. Hohn, T. Umehara, L. T. Guo, E. M. Osborne, J. Benner, C. J. Noren, J. Rinehart, and D. Soll. 2011. Expanding the genetic code of Escherichia coli with phosphoserine. *Science.* **333:** 1151–1154.
43. Soupene, E., V. Serikov, and F. A. Kuypers. 2008. Characterization of an acyl-coenzyme A binding protein predominantly expressed in human primitive progenitor cells. *J. Lipid Res.* **49:** 1103–1112.
44. Kishore, N. S., T. B. Lu, L. J. Knoll, A. Katoh, D. A. Rudnick, P. P. Mehta, B. Devadas, M. Huhn, J. L. Atwood, S. P. Adams, et al. 1991. The substrate specificity of Saccharomyces cerevisiae myristoyl-CoA:protein N-myristoyltransferase. Analysis of myristic acid analogs containing oxygen, sulfur, double bonds, triple bonds, and/or an aromatic residue. *J. Biol. Chem.* **266:** 8835–8855.

45. Towler, D. A., S. P. Adams, S. R. Eubanks, D. S. Towery, E. Jackson-Machelski, L. Glaser, and J. I. Gordon. 1987. Purification and characterization of yeast myristoyl CoA:protein N-myristoyltransferase. *Proc. Natl. Acad. Sci. USA.* **84:** 2708–2712.
46. Soupene, E., J. Rothschild, F. A. Kuypers, and D. Dean. 2012. Eukaryotic protein recruitment into the Chlamydia inclusion: implications for survival and growth. *PLoS One.* **7:** e36843.
47. Warncke, J. D., I. Vakonakis, and H. P. Beck. 2016. Plasmodium helical interspersed subtelomeric (PHIST) proteins, at the center of host cell remodeling. *Microbiol. Mol. Biol. Rev.* **80:** 905–927.
48. Filisetti, D., A. Theobald-Dietrich, N. Mahmoudi, J. Rudinger-Thirion, E. Candolfi, and M. Frugier. 2013. Aminoacylation of Plasmodium falciparum tRNA(Asn) and insights in the synthesis of asparagine repeats. *J. Biol. Chem.* **288:** 36361–36371.
49. Muralidharan, V., and D. E. Goldberg. 2013. Asparagine repeats in Plasmodium falciparum proteins: good for nothing? *PLoS Pathog.* **9:** e1003488.
50. Martin, D. D., E. Beauchamp, and L. G. Berthiaume. 2011. Post-translational myristoylation: fat matters in cellular life and death. *Biochimie.* **93:** 18–31.
51. Martin, D. D., and M. R. Hayden. 2015. Post-translational myristoylation at the cross roads of cell death, autophagy and neurodegeneration. *Biochem. Soc. Trans.* **43:** 229–234.
52. Aicart-Ramos, C., R. A. Valero, and I. Rodriguez-Crespo. 2011. Protein palmitoylation and subcellular trafficking. *Biochim. Biophys. Acta.* **1808:** 2981–2994.
53. Perinpanayagam, M. A., E. Beauchamp, D. D. Martin, J. Y. Sim, M. C. Yap, and L. G. Berthiaume. 2013. Regulation of co- and post-translational myristoylation of proteins during apoptosis: interplay of N-myristoyltransferases and caspases. *FASEB J.* **27:** 811–821.
54. Goncalves, V., J. A. Brannigan, E. Thinon, T. O. Olaleye, R. Serwa, S. Lanzarone, A. J. Wilkinson, E. W. Tate, and R. J. Leatherbarrow. 2012. A fluorescence-based assay for N-myristoyltransferase activity. *Anal. Biochem.* **421:** 342–344.
55. Rackham, M. D., J. A. Brannigan, D. K. Moss, Z. Yu, A. J. Wilkinson, A. A. Holder, E. W. Tate, and R. J. Leatherbarrow. 2013. Discovery of novel and ligand-efficient inhibitors of Plasmodium falciparum and Plasmodium vivax N-myristoyltransferase. *J. Med. Chem.* **56:** 371–375.